

Continental-scale joint inversion of Alaska and Yukon gravity and magnetic data

Martin Čuma^{1,2} and Michael S. Zhdanov^{1,2*} demonstrate how the moving sensitivity domain (MSD) approach combined with a large-scale parallelization makes it possible to simultaneously invert the gravity and magnetic data collected over large regional geological provinces.

Introduction

The 3D inversion of potential field data constitutes an increasingly important method of interpretation of geophysical data. A generalized inversion method first discretizes the 3D earth models into cells of constant density, susceptibility, or magnetization vector. In the case of continental-scale geophysical data collected by a combination of land, airborne and satellite measurements, the survey area may cover thousands and even millions of square kilometres, which makes the size of the inversion domain and the number of inverse model parameters extremely large. It is well known that for potential field data the computational complexity increases linearly with the size of the problem. Even a small-sized 3D inversion of huge amounts of data to 3D earth models with hundreds of thousands of cells can exceed the memory available on a desktop computer. In the case of several millions of discretization cells, the memory requirements may exceed the capacity even of the PC clusters. The second obstacle is the amount of

CPU time required to apply a huge, dense matrix of the forward modelling operator to the data and model vectors, even using parallel computing.

In order to overcome these difficulties, we have introduced the concept of a moving sensitivity domain (MSD) (Zhdanov and Cox, 2015; Zhdanov et al., 2014a, b). In the framework of this approach, for a given potential field receiver, we compute and store the Fréchet derivative matrix inside the inversion cells only within a predetermined horizontal distance from this receiver. The radius of the sensitivity domain (footprint) is selected based on the rate of the corresponding Green's function attenuation. For example, the footprint size for gravity fields is proportional to $1/r^2$; for gravity gradiometry and magnetic fields it is proportional to $1/r^3$; and for magnetic gradiometry it is proportional to $1/r^4$. It follows that the linear operators can be applied as sparse matrices with computational requirements reduced by several orders of magnitude and no loss of accuracy. In addition, our software

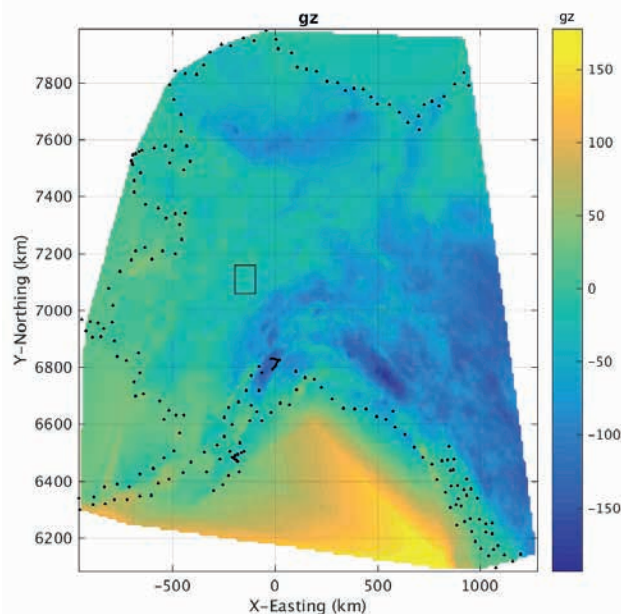


Figure 1 Map of the Bouguer Anomaly gravity data used in the inversion. The black dots denote the coast line, and the black box outlines the Minchumina Basin area analysed in more detail.

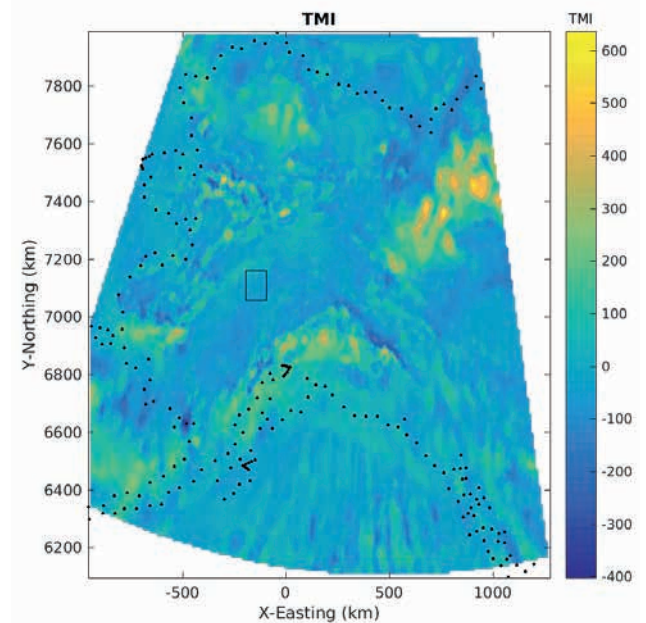


Figure 2 Map of the total magnetic intensity data used in the inversion. The black dots denote the coast line and the black box outlines the Minchumina Basin area analysed in more detail.

¹ TechnoImaging, Salt Lake City, USA | ² University of Utah, Salt Lake City, USA

* Corresponding author, E-mail: michael.zhdanov@utah.edu

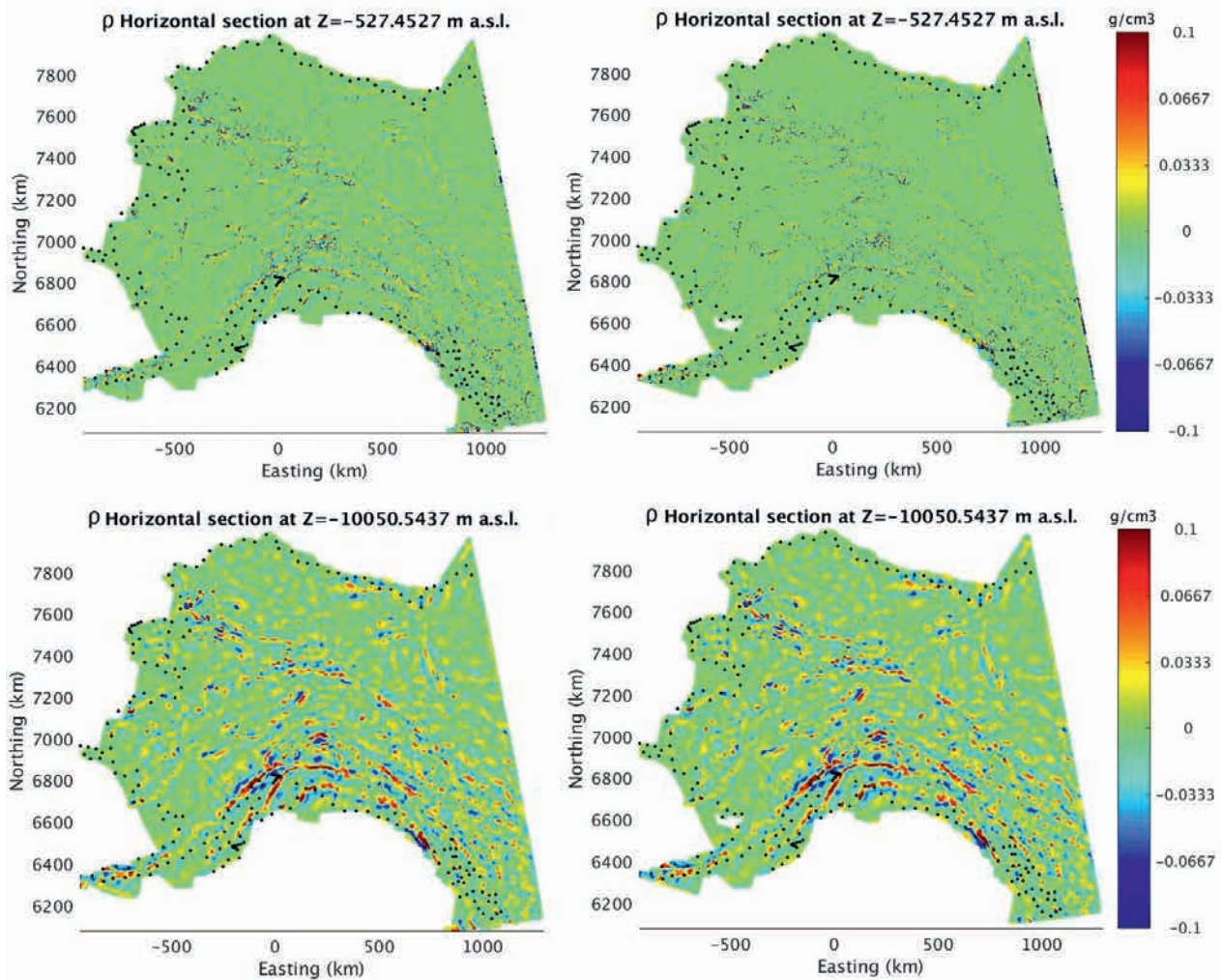


Figure 3 Horizontal cross sections of recovered density by separate (left panels) and joint (right panels) inversions at 500 m depth (upper two panels) and 10 km depth (lower two panels).

is fully parallelized so run times are in the order of hours on cluster resources. We have recently introduced a general method of solving truly large-scale potential field inverse problems with multi-level GPU parallelization where the modelling domain is discretized into hundreds of millions (even billions) of cells (Čuma and Zhdanov, 2014).

As gravity and magnetic inversion is an ill-posed problem, a regularization must be introduced to recover the most geologically plausible solutions from the infinite number of mathematically equivalent models. The regularization effectively selects the class of models from which a unique solution is sought. Over the years, a variety of methods have been developed for 3D inversion of potential field data with both smooth (e.g., Li and Oldenburg, 1996, 1998; Li, 2001) and focusing (e.g., Portniaguine and Zhdanov, 1999; Zhdanov, 2002, 2009, 2015) regularizations.

Non-uniqueness can also be reduced by incorporating additional information derived from available geological and/or geophysical data in the survey area to reduce the searching space for the solution. This additional information can be incorporated in the form of a joint inversion. Different geophysical fields provide information about the different physical properties of rock formations. In many cases this information is mutually

complementary, which makes it a natural for consideration in a joint inversion of the different geophysical data.

There are different approaches to joint inversion (see, for example, an excellent review by Dell'Aversana, 2013). In a case where the corresponding model parameters are identical or mutually correlated, the joint inversion can explore the existence of this known correlation (e.g., Jupp and Vozoff, 1975; Hoversten et al., 2003, 2006). In a case, where the model parameters are not correlated, but nevertheless have similar geometrical features, the joint inversion can be based on structure-coupled constraints. It is often based on minimizing a value of the cross gradients between different model parameters. This has now been widely used in the joint inversion of geophysical data (e.g., Colombo and De Stefano, 2007; Hu et al., 2009; Jegen et al., 2009; De Stefano et al., 2011; Moorkamp et al., 2011). Zhdanov et al. (2012) developed a generalized approach to joint inversion based on Gramian constraints which correlate and/or impose structural similarities between different physical properties without a priori knowledge about a specific form of these cross-model relationships (for details, see Zhdanov, 2015). The principles of joint inversion of gravity and magnetic data using Gramian constraints was also outlined in a paper published in *First Break* last year (Zhdanov et al., 2016).

In this paper, we present a case study of a continental-scale joint inversion of gravity and magnetic data covering the US state of Alaska and Canadian province of Yukon using parallel GPU capable software (Čuma and Zhdanov, 2014).

The sources of the data and their preparation for inversion

Apart from specific ground-based and airborne surveys, both gravity and magnetic data are also available as global products with the base data typically obtained by satellite observations and augmented with ground or airborne data, where available.

The Alaska gravity data are based on the ground-based measurements from USGS, with the total of 91,547 stations covering the area of approximately 1,800,000 km². The Yukon Gravity data came from Natural Resources Canada, totalling 12,211 stations distributed over an area of approximately 500,000 km². The Complete Bouguer Anomaly data were converted from the original NAD83_Albers_Alaska coordinates to the UTM Cartesian co-ordinates (UTM zone 7) and interpolated into a 1 km × 1 km grid resulting in 2,504,665 data points. These gravity data were then processed with a high-pass filter with cut-off of 10,000 m to remove regional effects.

Magnetic data in the form of total magnetic intensity are available globally through a number of products that include contributions from the Earth's core, crust and/or ionosphere. As in this geophysical inversion we are mainly interested in the crustal anomalies, we chose the EMAG2_V3 model (Meyer et al., 2016), which is compiled from satellite, ship, and airborne magnetic measurements and delivered on a 2 arc-minute grid (approximately 2 km) in WGS94 co-ordinate system. We extracted the data covering the area of Alaska and Yukon and converted to the UTM Cartesian grid (UTM zone 7). The data were continued upward to an elevation of 4 km; thus, we used a 4-km observation point height for the magnetic data throughout the inversion. This upward continuation limits the near-surface resolution of the magnetic data.

For magnetic modelling, we also need the value of the reference magnetic field. For this, we used the IGRF-12 geomagnetic model (Thébault et al., 2015). As the geomagnetic model varies with distance, which can be considerable on a continental scale, we modified our modelling algorithm to use a unique IGRF value for each observation point. The reference magnetic field varies with time as well, so we selected 1/1/2016 as the reference date, which roughly corresponds to the publishing date of the

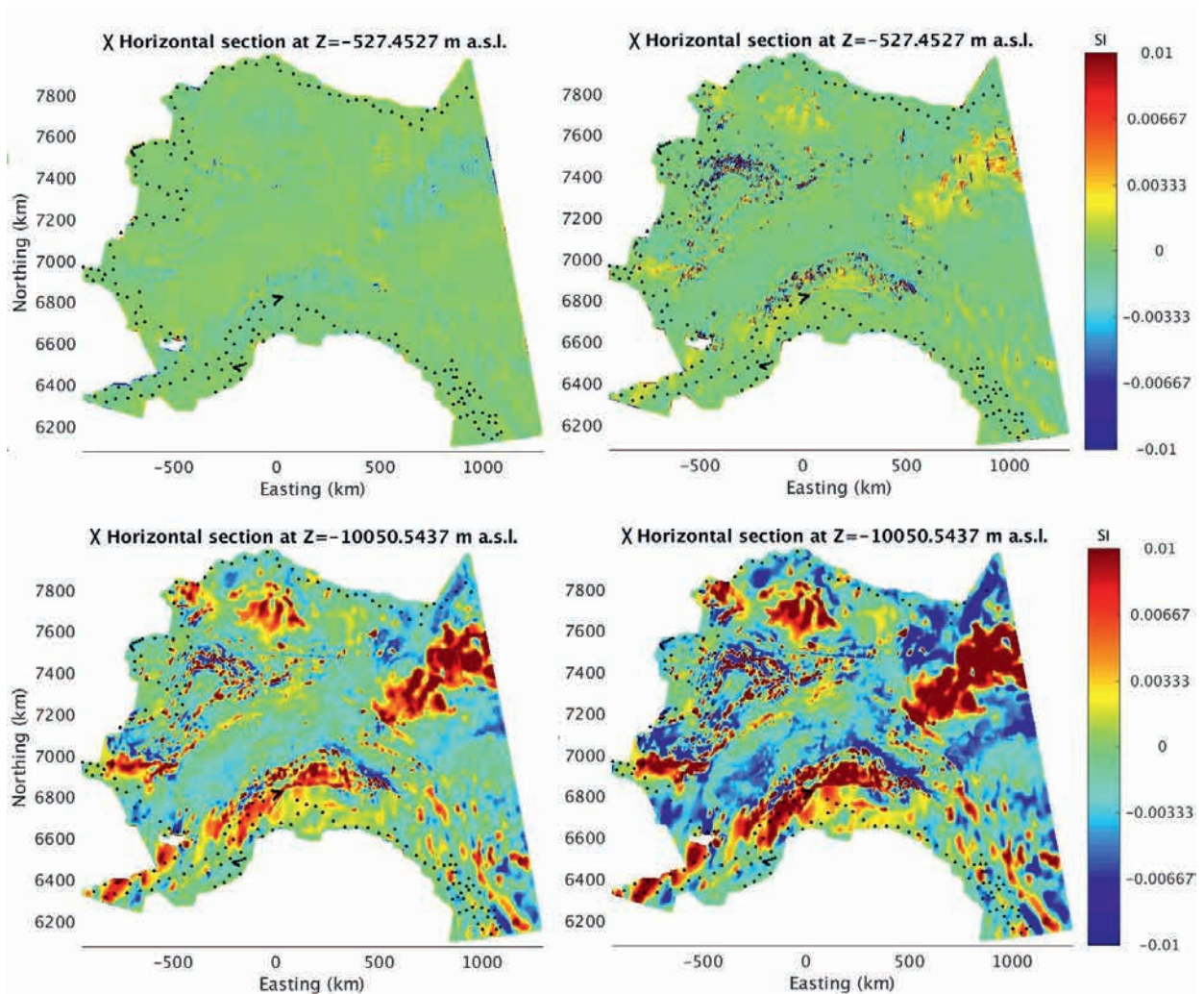


Figure 4 Horizontal cross-sections of recovered susceptibility by separate (left panels) and joint (right panels) inversions at 500 m depth (upper two panels) and 10 km depth (lower two panels).

EMAG_V3 magnetic model. The maps of gravity and magnetic data used in this study are shown in Figures 1 and 2.

Results

The TMI data used for the inversion were presented roughly on a 2-km grid while the gravity data were taken on a 1-km grid. Both datasets were cut on the sides of the survey area to approximately copy the landmass surface. For both independent and joint inversions on the continental scale we have discretised the inversion domain using a 2-km horizontal grid. For the vertical discretization, we started with a 200 m vertical cell size and increased it by 3% at every horizontal layer up to total depth of the inversion domain of 27 km. This resulted in ca. 60 million domain cells and ca. 626,000 data points for the gravity and 420,000 data points for the TMI data. We ran all the inversions with our parallel OpenACC GPU enabled program (Čuma and Zhdanov, 2014). Note that we considered the effect of the Earth’s curvature by incorporating simple geometric correction terms in the potential fields modelling kernels (Lane, 2009).

We first conducted the independent inversions of gravity and TMI data, and then proceeded to run a joint inversion of

the gravity and TMI data over the entire region. For the joint inversion, we used the same grid as in the separate inversions, i.e. 2×2 km horizontal cell size and 200 m vertical cell size at the surface increasing by 3% at every layer up to a total depth of 27 km. The inversion for roughly 60 million cells and 1 million data points took about three days to complete on nine dual GPU nodes equipped with NVidia Tesla M2090 cards. We used a single Gramian stabilizer for the entire inversion domain enforcing a correlation between density and susceptibility. We ran both the separate and joint inversions to a common L_2 norm misfit of 1%, which took 30 iterations for TMI data, 70 for gravity data, and 70 iterations for the joint inversion, respectively.

The inversion results consist of two extremely large-scale 3D models of the Earth’s crust, distributions of the density and magnetic susceptibility. They span an area of approximately 2,300,000 km² covering Alaska and Yukon, and extending at a depth of 27 km. Figures 3 and 4 show horizontal cross sections of density and susceptibility obtained with separate and joint continental-scale inversions at 500 m depth (upper two panels) and 10 km depth (lower two panels). We should note that the differences between the results of the separate and joint inversions for the density distribution are relatively small and difficult to see

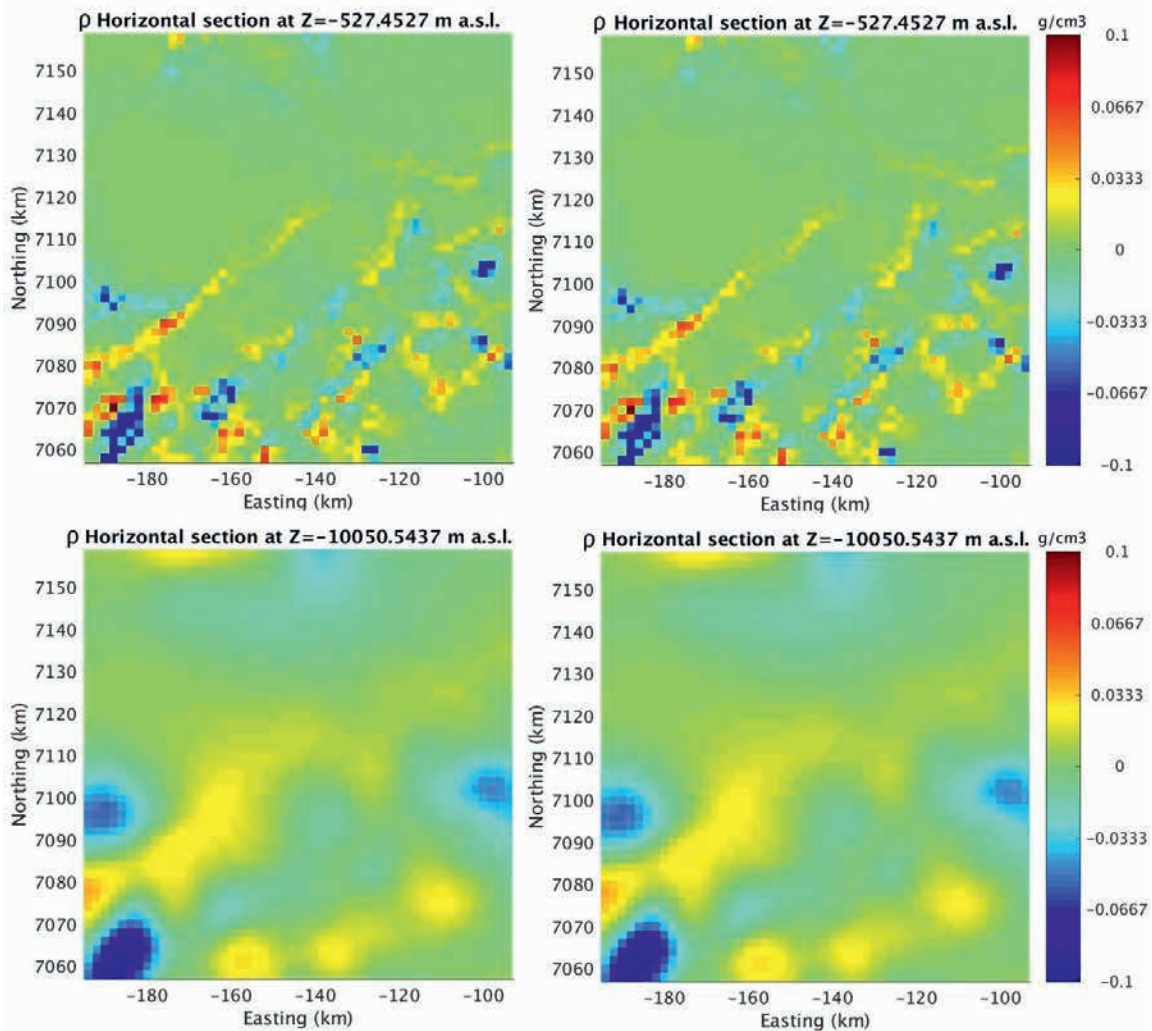


Figure 5 Minchumina Basin area: horizontal cross sections of density recovered by the independent continental-scale inversion (left panels) and joint continental-scale inversion (right panels) at 500 m depth (upper panels) and 10 km depth (lower panels).

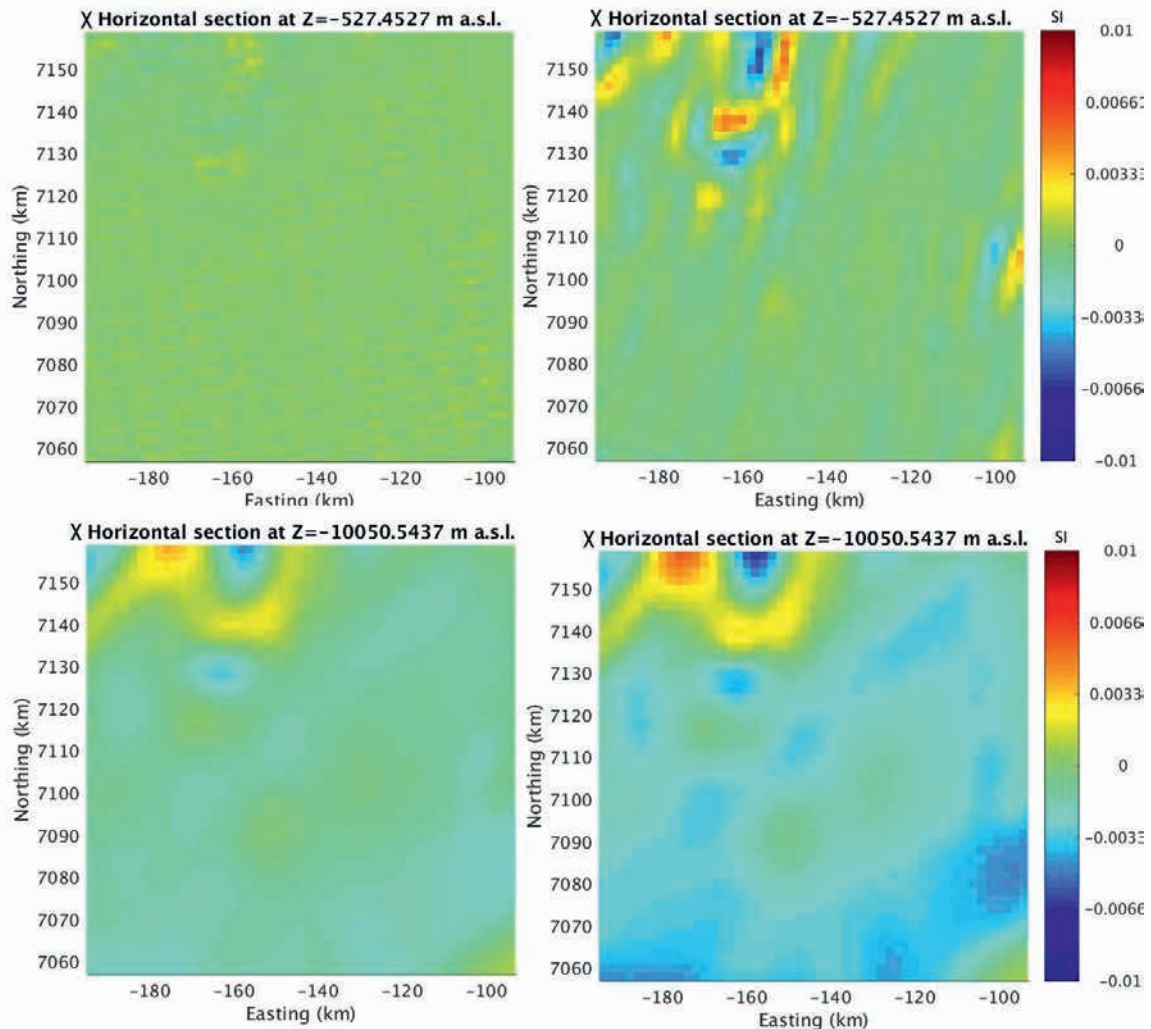


Figure 6 Minchumina Basin area: horizontal cross-sections of susceptibility recovered by the independent continental-scale inversion (left panels) and joint continental-scale inversion (right panels) at 500 m depth (upper panels) and 10 km depth (lower panels).

owing to the large scale of the inversion domain. However, the differences in magnetic properties distribution are quite visible in these maps. The produced 3D models of density and susceptibility distribution in Alaska and Yukon provide invaluable information about the geology of this vast region. These models can be used as a foundation of geological and structural interpretation of geophysical data on a continental scale, which will serve as a road map for future mineral exploration.

To assess the utility of continental-scale inversion for regional anomaly exploration, and to evaluate the effect of density and susceptibility coupling at a reasonably observable scale, we also focused on a small section of ca. 100×100 km² in the Minchumina Basin in central Alaska. There is a number of underexplored basins in Alaska that have hydrocarbon potential, and this is one of them. We ran this regional-scale inversion on 500×500 m² horizontal cell size and vertical size starting with 150 m and increasing by 3% up to the depth of 27 km. In this basin, the correlation between density and susceptibility is strong, and therefore we can use the strength of the Gramian stabilizer. As in the full domain case, we ran the inversion to a normalized L_2 norm misfit of 1%.

In Figures 5 and 6 we compare the results of the separate and joint inversions of the Minchumina Basin subset for a few hori-

zontal cross-sections, obtained from the continental-scale inversions. The density maps shown in the figures are similar between the separate and joint inversion, but we observe noticeable focusing of the susceptibility, particularly near the surface. For these particular upward continued TMI data, the main utility of the joint inversion is the considerably improved susceptibility resolution at the near surface. In Figures 7 and 8 we compare the regional-scale inversion result with a cut-off of the continental-scale inversion discussed above. The correlation of the continental-scale result with the regional-scale inverse model is fairly good, despite a weak enforcement of the coupling between the density and the susceptibility at the continental-scale inversion. The cross plots of density and susceptibility for the models obtained from the regional inversions are shown in Figure 9. We notice a stronger correlation trend in the joint inversion result (right panel) owing to the stronger weight of the Gramian stabilizer, which suggests the presence of a linear trend in this area.

Conclusions

We have developed a computationally effective algorithm of joint inversion of the gravity and magnetic data on a continental scale based on a Gramian stabilizer. The extremely large-scale

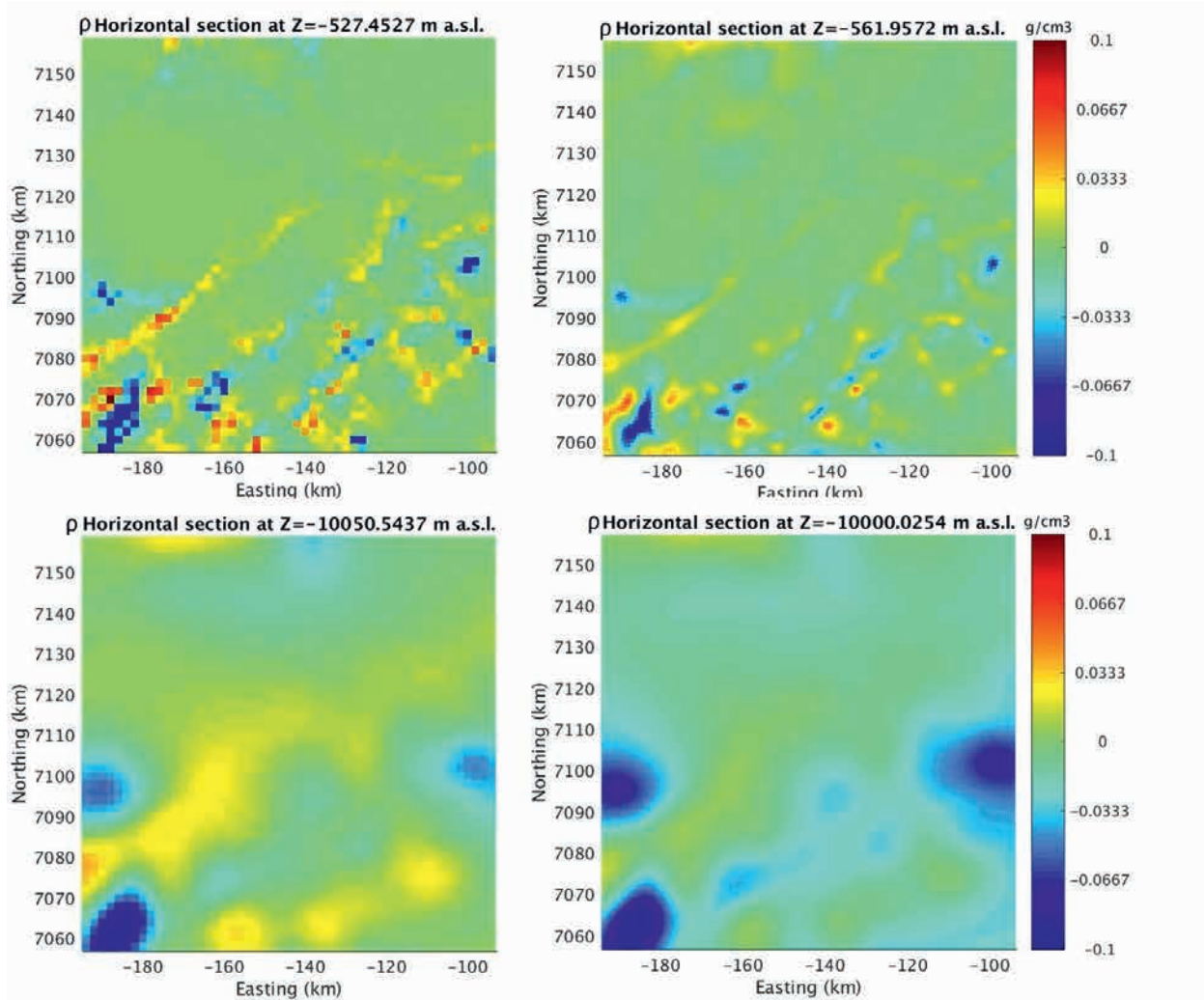


Figure 7 Minchumina Basin area: horizontal cross sections of density recovered by the continental scale inversion (left panels) and regional inversion (right panels) at 500 m depth (upper panels) and 10 km depth (lower panels).

inversion was made possible by developing a fully parallelized and GPU accelerated modelling and inversion implemented using a moving sensitivity domain approach.

The developed algorithm was applied to the gravity and magnetic data collected over the US state of Alaska and the Canadian province of Yukon, covering the area of approximately 2,300,000 km². In the joint continental-scale inversion, we did not expect to recover a strong uniform correlation between density and susceptibility over the entire area of Alaska and Yukon with a single Gramian relationship. However, more localized areas were found where a single dependence between density and susceptibility existed, as we demonstrated in the case of the Minchumina Basin. The joint inversion also improved the near-surface resolution of the upward continued magnetic data. The utility of a joint inversion approach on a continental scale lies in a single coupled density and susceptibility model of the whole continent, where a geoscientist can focus on areas of geological interest without the need to perform separate inversions on these areas. We have demonstrated this utility by comparing the cut-out of Minchumina Basin continental-scale result with a regional-scale inverse model and found them very similar.

The produced 3D models of density and susceptibility distributions in Alaska and Yukon provide invaluable information

about the geology of this vast region. These models can be used as a foundation of geological and structural analysis of geophysical data on a continental scale, which will serve as a road map for future mineral, oil, and gas exploration. The in-depth geological interpretation of these large-scale models will constitute a subject of future research.

Acknowledgements

The authors acknowledge the support of TechnoImaging and the University of Utah Consortium for Electromagnetic Modelling and Inversion (CEMI). We also acknowledge allocation of computer time provided by the University of Utah's Centre for High Performance Computing (CHPC).

References

Colombo, D. and De Stefano, M. [2007]. Geophysical modeling via simultaneous joint inversion of seismic, gravity, and electromagnetic data: Application to prestack depth imaging. *The Leading Edge*, **26**, 326-331.

Čuma, M. and Zhdanov, M.S. [2014]. Massively parallel regularized 3D inversion of potential fields on CPUs and GPUs. *Computers and Geosciences*, **62**, 80-87.

Dell'Aversana, P. [2013]. *Cognition in Geosciences*. EAGE Publications, Houten, The Netherlands.

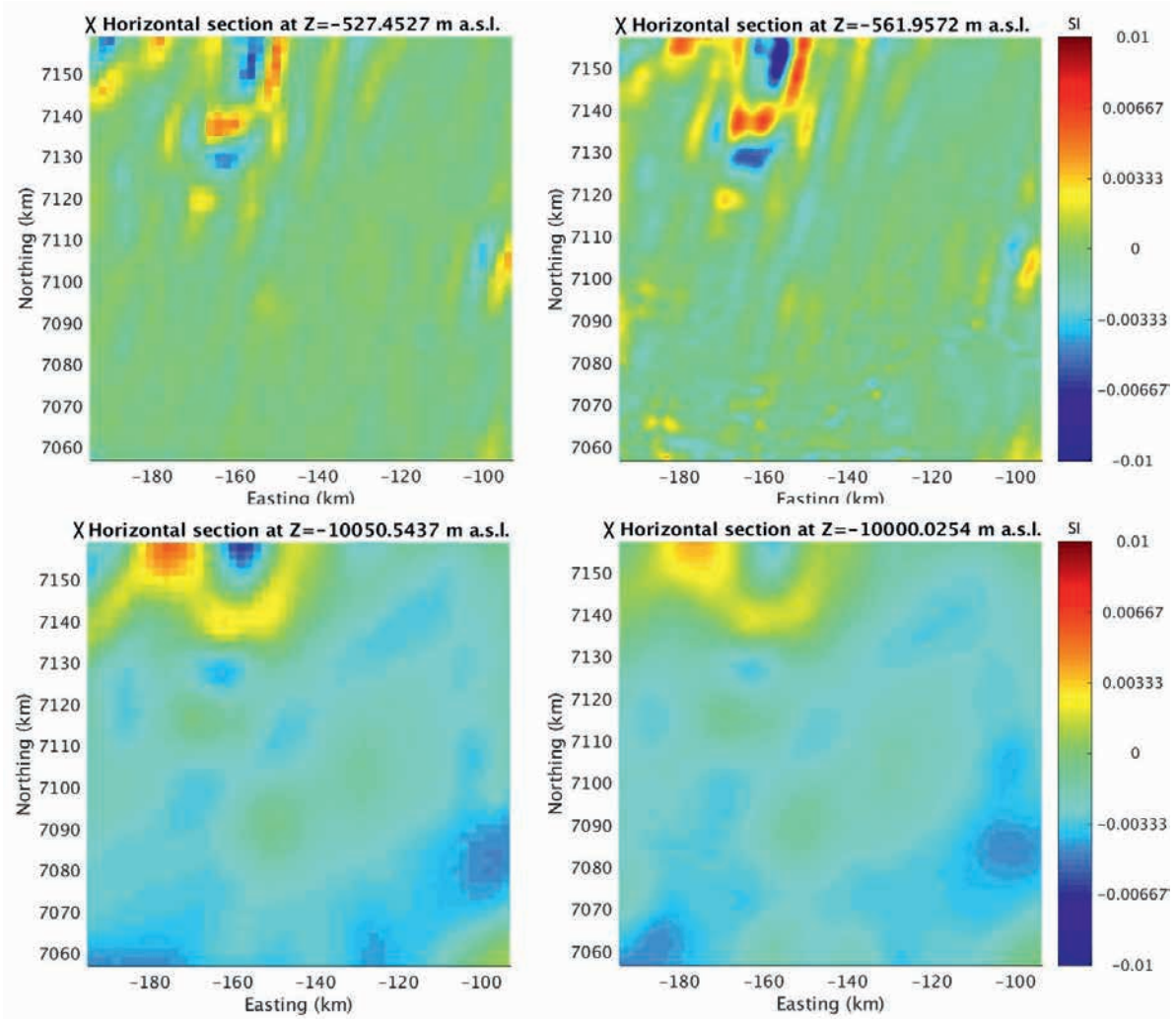


Figure 8 Minchumina Basin area: horizontal cross sections of susceptibility recovered by the continental scale inversion (left panels) and regional inversion (right panels) at 500 m depth (upper panels) and 10 km depth (lower panels).

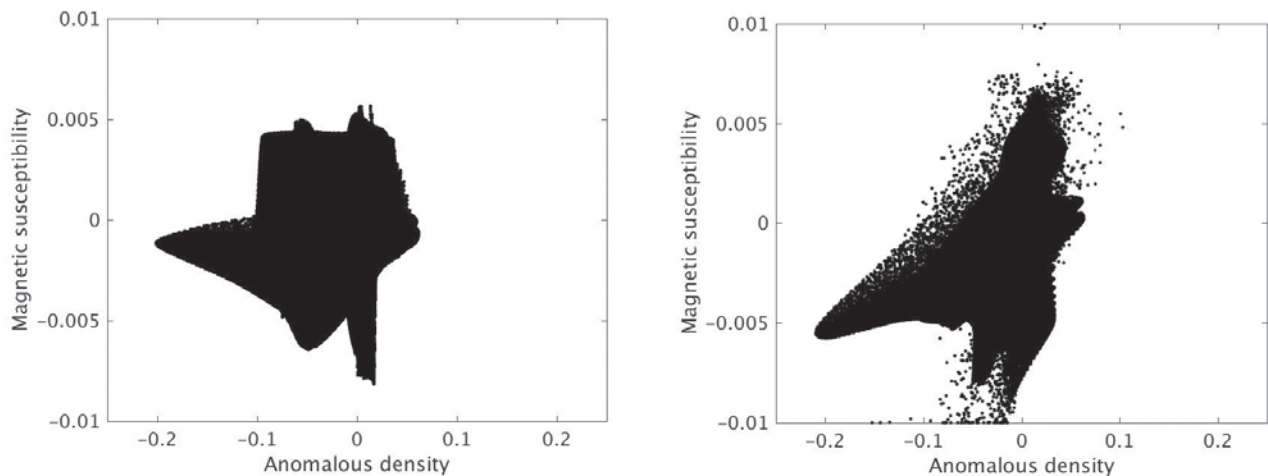


Figure 9 Cross plots of density vs. susceptibility for the independent regional-scale inversion (left panel) and joint regional-scale inversion (right panel).

Hoversten, G.M., Gritto, R., Washbourne, J. and Daley, T. [2003]. Pressure and fluid saturation prediction in a multicomponent reservoir using combined seismic and electromagnetic imaging. *Geophysics*, **68**, 1580-1591.

Hoversten, G.M., Cassassuce, F., Gasperikova, E., Newman, G.A., Chen, J., Rubin, Y., Hou, Z. and Vasco, D. [2006]. Direct reservoir parameter estimation using joint inversion of marine

seismic AVA and CSEM data. *Geophysics*, **71**, C1-C13.

Hu, W.Y., Abubakar, A. and Habashy, T.M. [2009]. Joint electromagnetic and seismic inversion using structural constraints. *Geophysics*, **74**, R99-R109.

Jupp, D.L.B. and Vozoff, K. [1975]. Joint inversion of geophysical data. *Geophysical Journal of the Royal Astronomical Society*, **42**, 977-991.

Jegen, M.D., Hobbs, R.W., Tarits, P. and Chave, A. [2009]. Joint inversion of marine magnetotelluric and gravity data incorporating seismic constraints: Preliminary results of sub-basalt imaging off the Faroe Shelf. *Earth and Planetary Science Letters*, **282**, 47-55.

Lane, R. [2009]. Some issues and insights for gravity and magnetic modeling at the region to continent scale: *ASEG*, Extended Abstracts.

Li, Y. and Oldenburg, D.W. [1996]. 3-D inversion of magnetic data. *Geophysics*, **61**, 394-408, doi: 10.1190/1.1443968.

Li, Y. and Oldenburg, D.W. [1998]. 3-D inversion of gravity data. *Geophysics*, **63**, 109-119, doi: 10.1190/1.1444302.

Li, Y. and Oldenburg, D.W. [2003]. Fast inversion of large-scale magnetic data using wavelet transforms and a logarithmic barrier method. *Geophysical Journal International*, **152**, 251-265, doi: 10.1046/j.1365-246X.2003.01766.

Meyer, B., Saltus, R. and Chulliat, A. [2016]. EMAG2: Earth Magnetic Anomaly Grid (2-arc-minute resolution) Version 3: National Centers for Environmental Information, NOAA. doi:10.7289/V5H70CVX [access date 1/15/2017].

Moorkamp, M., Heincke, B., Jegen, M., Robert, A.W. and Hobbs, R.W. [2011]. A framework for 3-D joint inversion of MT, gravity and seismic refraction data. *Geophysical Journal International*, **184**, 477-493.

Portniaguine O. and Zhdanov, M.S. [1999]. Focusing geophysical inversion images. *Geophysics*, **64**, 874-887, doi: 10.1190/1.1444596.

Thébault, E., C.C. Finlay, C.D. Beggan, P. Alken, J. Aubert, O. Barrois, F. Bertrand, T. Bondar, A. Boness, L. Brocco, E. Canet, A. Chambodut, A. Chulliat, P. CoÅsson, F. Civet, A. Du, A. Fournier, I. Fratter, N. Gillet, B. Hamilton, M. Hamoudi, G. Hulot, T. Jager, M. Korte,

W. Kuang, X. Lalanne, B. Langlais, J.-M. LaCreger, V. Lesur, F.J. Lowes [2015]. International Geomagnetic Reference Field: the 12th generation. *Earth, Planets and Space*, 67-79.

Zhdanov, M.S. [2002]. Geophysical inverse theory and regularization problems: Elsevier.

Zhdanov, M.S. [2009]. New advances in 3D regularized inversion of gravity and electromagnetic data. *Geophysical Prospecting*, **57** (4), 463-478, doi: 10.1111/j.1365-2478.2008.00763.x.

Zhdanov, M.S. [2015]. *Inverse theory and applications in geophysics*. Elsevier.

Zhdanov, M.S., Gribenko, M.V. and Wilson, G. [2012]. Generalized joint inversion of multimodal geophysical data using Gramian constraints. *Geophysical Research Letters*, **39**, L09301, 1-7.

Zhdanov, M.S., and Cox, L. [2015]. Method of subsurface imaging using superposition of sensor sensitivities from geophysical data acquisition systems. U. S. Patent US 2013/0173163.

Zhdanov, M.S., Endo, M., Cox, L.H., Čuma, M. Linfoot, M., Anderson, C., Black, A. and Gribenko, A.V. [2014a]. Three dimensional inversion of towed streamer electromagnetic data. *Geophysical Prospecting*, **62** (3), 552-572, doi: 10.1111/1365-2478.12097.

Zhdanov, M.S., Endo, M., Yoon, D., Čuma, C., Mattsson, J. and Midgley, J. [2014b]. Anisotropic 3D inversion of towed-streamer electromagnetic data: Case study from the Troll West oil province. Interpretation, **2** (3), SH97-SH113, doi: 10.1190/INT-2013-0156.1.

Zhdanov, M.S., Zhu, Y., Endo, M., and Kinakin, Y. [2016]. Novel approach to joint 3D inversion of EM and potential field data using Gramian constraints. *First Break*, **34** (4), 59-64.

ADVERTISEMENT

Featuring the highly anticipated Technical Gurus at APGCE 2017



Prof Paul Tapponnier
Professor
Earth Observatory of Singapore,
Singapore.



Prof Robert Hall
Professor and Director of SE Asia Group,
Royal Holloway University of London,
United Kingdom.



Ian Longley
Geologist/Director,
GIS-PAX Ltd.,
Australia.



Dries Gisolf
Director,
R&D, Delft Inversion,
Netherlands.



Prof Richard Swarbrick
Managing Director,
Swarbrick GeoPressure Consultancy Ltd.,
United Kingdom.



Prof Don Lawton
Director,
Containment and Monitoring
Institute at Carbon Management,
University of Calgary, Canada.

REGISTER NOW at www.apgce.com

ASIA PETROLEUM GEOSCIENCE CONFERENCE & EXHIBITION (APGCE) 2017

Collaborative Solutions. Sharing Success.

20-21 NOVEMBER 2017

Kuala Lumpur Convention Centre, Malaysia



Hosted by:



Event Organiser: In collaboration with:



apgce@icep.com.my

@APGCE2017

@apgce2017